Enhancing Microstructure, Grain Refinement, and Wear Properties of Cast A356-TiB_2 Composite through Improved Sequence of ECAP and Heat Treatment Processes

M. Syukron [a], A.S. Anasyida [b,*], H. Zuhailawati [b], M.H. Hassan [c], B.K. Dhindaw [d], S.A. Zakaria [b], T.E. Abioye [b,e]

[a] Metallurgical Engineering, Faculty of Mineral Technology, Universitas Pembangunan Nasional "Veteran" Yogyakarta, Indonesia
[b] School of Materials & Mineral Resources Engineering, Universiti Sains Malaysia, Penang, Malaysia
[c] School of Mechanical Engineering, Universiti Sains Malaysia, Penang, Malaysia
[d] Indian Institute of Technology Kharagpur, India
[e] Industrial and Production Engineering Department, School of Engineering and Engineering Technology, Federal University of Technology Akure, Akure, Ondo State, Nigeria

Corresponding author: A.S.Anasyida
email: anasyida@usm.my

(Received 11 January 2024; Accepted 16 December 2024)

Abstract
This study aimed to enhance the grain structure, hardness, and wear resistance of A356-1.5TiB_2 composite through a combination of manufacturing processes. Initially, the composite was produced using casting, followed by equal channel angular pressing (ECAP) and heat treatments in various sequences. The heat treatment process involved a solution heat treatment (540ºC, 4 hours), followed by rapid quenching in water (90ºC). The ECAP process was carried out via the BA route, involving four passes at room temperature. After ECAP, an aging process was conducted at 155ºC for 3 hours. The post-application of ECAP and heat treatments had a positive impact on the distribution of TiB_2 and $TiAl_3$ particles, aluminum matrix grain refinement, and improved hardness and wear properties of the composite. The composite underwent both ECAP and heat treatment exhibited finer grain structure and higher hardness. The sequence of post-applications of ECAP and heat treatments also affected the grain structure, hardness, and wear resistance of the composite. The composite that underwent solution treatment followed by aging treatment and then ECAP demonstrated the most refined structure and highest hardness. These findings demonstrate that a carefully designed manufacturing process can significantly enhance the mechanical properties of A356-1.5TiB_2 composite.

Keywords: aluminium metal matrix composite; grain structure, equal channel angular pressing (ECAP); heat treatment: hardness; wear

1, Introduction

Compared with aluminium alloys, aluminium metal matrix composites (AMMCs) have higher potential for industrial applications especially, where high-strength-wear resistance properties

coupled with lightweight are required. The increasing global demand for AMMCs is due to their excellent combination of superior elastic modulus, excellent specific strength, light weight, high stiffness, and enhanced wear resistance [1,2]. Hard ceramic particles such as WC, B_4C, TiO_2, $ZrSiO_4$, TiC, SiC, ZrO_2, TiB_2, Si_3N_4, Al_2O_3 and ZrB_2 are often used to reinforce aluminium alloys to fabricate AMMCs [3-8]. Among the reinforcement, TiB_2 possesses effective combination of physical and mechanical properties such as high thermal stability, high strength, high heat conductivity, low density, superior hardness, oxidation stability, and high resistance to mechanical erosion [9].

Al–5Ti–B master alloy was used as grain refiner in the casting of aluminium alloys because it is a source of TiB_2 and Al_3Ti which favours grain refinement [10]. Guzowski et al. [11] stated that the Al_3Ti and TiB_2 particles are respectively located at the grain center and boundary, suggesting that the (Al, Ti)B_2 particles are the preferred nucleation sites. Therefore, reinforcing aluminum alloy with TiB_2 is good for enhanced microstructure and mechanical properties. However, the issue of concern is the agglomeration of the reinforcement particles which is detrimental to the mechanical properties hence, service performance of the developed composite [12]. One of the means of preventing particles agglomeration and enhancing grain refinement during casting of aluminium composites is to ensure fragmentation of the reinforcement particles into smaller sizes by applying high strain deformation. The incorporation of high strain deformation can provide value-added and more refined cast structure products which can be used for more critical applications.

Equal-channel angular pressing (ECAP) has been established as a promising severe plastic deformation (SPD) technique that produces high strain and enhances grain refining performance of master aluminium alloys (grain refiners) [13, 14, 15]. For example, the effects of the ECAP on the microstructure and grain refining performance of Al-5%Ti master alloy and its subsequent effects on the hardness of pure aluminium have been investigated by Wei et al [16]. It was found that the grain refining ability of the Al-5%Ti master alloy processed by ECAP was better than those without ECAP. Also, the hardness of pure aluminium cast samples increased because of the addition of Al–5%Ti master alloy processed by ECAP. Enhancement of the grain refinement efficiency of Al-B master alloy processed by ECAP has also been investigated by Wei et al. [17]. It was discovered that the grain size of AlB_2 reduced significantly from about 34 μm to approximately 12 μm after 4 ECAP passes. This proved an increase in the refining performance and fading resistance of Al-3% B master alloy on a commercially pure aluminium. Zhang et al. [18] testified that the mean size of TiC and Al_3Ti particles decreased in Al-5%Ti-0.25%C alloy after ECAP compared with that before ECAP, indicating a double grain refining effect.

Chidambaram et al. [19] studied microstructure and mechanical properties of AA6061–5wt. %TiB_2 in-situ metal matrix composite subjected to ECAP. The result showed an improvement in strength and Vickers hardness due to the grain refinement and redistribution of in-situ TiB_2 particles in the aluminium matrix. Also, Chidambaram et al. [20] had established that the number of ECAP passes has significant influence on the wear resistance of ECAP processed AA6061 and ECAP processed AA6061-TiB_2 with the highest wear resistance found at 6 ECAP passes. The ECAP passes affects the bonding between TiB_2 and Al matrix.

Moreover, the combined effects of the heat treatment processes and SPD via ECAP on the mechanical and wear properties of cast aluminium metal matrix composites have also been

investigated. The evaluation of the mechanical performance of ECAP processed AA6061/TiB2 composites with and without prior pre-heat treatments (T4 and then T6) has been investigated by Shobha et al. [21]. It was found that the heat treated in-situ Al-TiB_2 composite subjected to SPD via ECAP exhibited a more refined microstructure which explained the better mechanical properties demonstrated by the composite. The heat treated in-situ Al-TiB_2 composite subjected to SPD via ECAP also exhibited higher hardness and wear resistance than the Al-TiB_2 composite subjected to SPD without heat treatment. Lokesh and Mallik [22] had investigated the microstructure and mechanical properties of AA6061-Gr cast composites subjected to solution annealing treatment before undergoing SPD via ECAP. The reinforcement particles were homogeneously distributed in the aluminium matrix which has its grain size significantly reduced after the heat treatment and ECAP processes. This translated to remarkable higher performance of the heat-treated and then ECAP processed composite sample in terms of hardness and ultimate tensile strength compared with the base AA6061 alloy and as-cast AA6061-Gr composite.

So far, various efforts including application of SPD via ECAP, variation of ECAP pass and combination of heat treatments and ECAP processes have been geared towards enhancing the grain refinement (i.e. microstructure), wear and mechanical properties of AMMCs. Though the combined effects of heat-treatment and ECAP processes produced a more significant improvement, investigation on combination manufacturing process sequence of heat treatment and ECAP processes will affect the microstructure, hardness, and wear properties of cast AMMCs is still scanty in the literature. As a result, the current study aims at determining combination manufacturing process sequence of heat treatment and ECAP for enhancing the grain structure, hardness, and wear properties of A356-TiB_2 composite.

2. Experimental Procedures

The materials used for casting in this work include pure Al, pure Mg, pure Si and Al-5Ti-1B master alloy. Also, A356 (AlSiMg) alloy with nominal composition (wt.%) of Al-92, Si-7, Mg-0.35, Fe-0.2, Cu-0.2 and Zn-0.1 was obtained for reference. The weight ratio of cast materials (i.e., pure Al, pure Mg, pure Si and Al-5Ti-1B master alloy) was calculated to get the targeted cast composition for A356 alloy and A356-1.5 wt.% TiB_2 composite. The samples were prepared through melting and casting route. The mixtures were melted in graphite crucibles at 850 °C in an electric melting furnace, and the melted alloys were cast in steel mold to create castings of 14 mm in diameter and 70 mm in length. Thereafter, the cast composite samples were solution heat treated by maintaining them at 540°C for 4 h, followed by rapid quenching in water at 90°C to prevent cracking [17].

The cast composite samples underwent aging heat treatment and 4-pass ECAP processes, depending on the specific manufacturing process combination listed in Table 1. These treatments were carried out to enhance the grain structure and wear resistance properties of the samples. Figure 1 shows a schematic of the solution treatment, quenching, and aging method used, with aging being performed at a soaking temperature of 155ºC for 3 hours. To prepare the samples for the ECAP process, the surface was ground using SiC paper with 600 and 1200 grit to achieve a smooth surface and minimize friction between the sample and the walls of the ECAP mould. ECAP processing was conducted at room temperature with a pressing speed of 2.4 mm/min using a die with $\phi = 120^{\circ}$, and the outer angle of the channel intersection is neglected due to a sharp corner as indicated in Figure 2. The ECAP process cycle was repeated four times to achieve 4-pass ECAP via B_A route (the sample was rotated 90º clockwise and counter-clockwise alternatively).

Table 1 *Process sequence of aging heat treatment and ECAP carried out on cast A356-1.5TiB$_2$ composite*

No	Sample labels	Manufacturing sequence process
1.	ST-ECAP	Solution treatment + 4-pass ECAP.
2.	ST-Aging-ECAP	Solution treatment + Aging treatment + 4-pass ECAP
3.	ST-ECAP-Aging	Solution treatment + 4-pass ECAP + Aging treatment

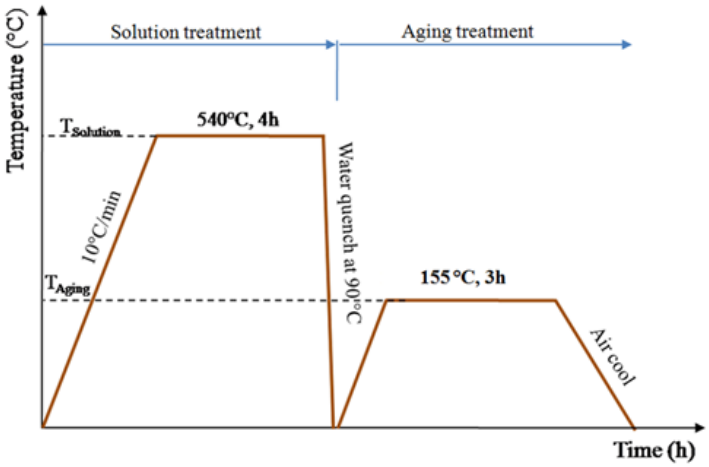

Figure 1. *Heat treatment profile*

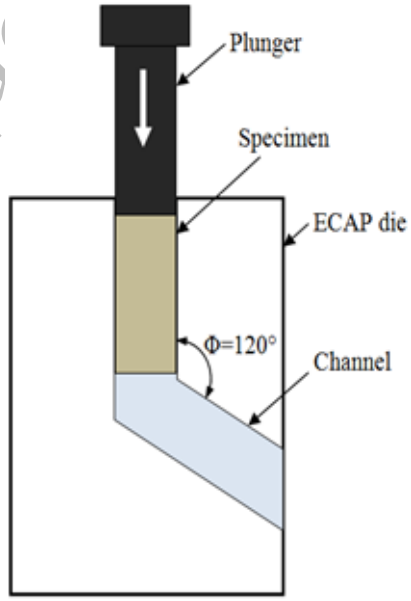

Figure 2. *Sketch of ECAP processing*

Thereafter, all the samples were polished and etched in hydrofluoric acid (0.5 ml) and deionized water (99.5 ml) reagent for 15 s. The microstructures were characterized by an Olympus optical microscope equipped with an image analyzer (IA), field emission scanning electron microscope (FESEM) model Gemini SUPRA 35VP and high-resolution transmission electron microscopy (HRTEM) model Tecnai F200. Grain size and misorientation angle of the grains were studied using OM (intercept method) and EBSD (FESEM, JEOL JSM-7001FA).

The wear test was conducted using a tribotester pin-on-disc wear-testing machine (TR 20 DUCOM) equipped with WinDucom software. The dry sliding wear behavior of the samples against a hardened (RC60) carbon steel EN-31 (Fe-2.3%Cr-0.9%C) disc was investigated according to ASTM G99. The wear test was conducted at a fixed speed of 1 m/s with loads of 30 and 50 N for sliding distance up to 5 km. The wear test was conducted in dry conditions at room temperature. The test is interrupted for measurement at 1 km, 2 km, 3 km, 4 km, and 5 km sliding distances. The weight loss of the pin material was calculated by measuring weigh before ($W1$) and weight after ($W2$) using a digital weight balance up to accuracy of 0.0001 g. Volume loss and the specific wear rate were calculated using Eq. (1) and Eq. (2), respectively [23].

$$V_L = \frac{(\Delta W \times 1000)}{\rho} \tag{1}$$

$$S_{WR} = \frac{V_L}{N \times S} \tag{2}$$

Where V_L is the volume loss (mm^3); S_{WR}, the specific wear rate (mm^3/N m); ΔW, the weight loss = ($W1–W2$); ρ, the density (g/cm^3); N, the applied load (N); and S, the sliding distance (m). Friction coefficient values under steady state were calculated by the load attached equipped with the apparatus. The worn surfaces were observed using FESEM (SURPA 35VP ZEISS) equipped with an additional Energy Dispersive X-Ray (EDX) detector.

3. Results and Discussion

3.1 Microstructural characterization

The optical micrographs and SEM images of as-cast A356 aluminum alloy and A356-1.5TiB_2 composite are shown in Figure 3. The microstructure of the as-cast A356 aluminium alloy (see Figure 3a and 3b) comprised mainly of two phases which are α-Al dendrites (i.e. the continuous dark contrast matrix) and eutectic Si (i.e. white contrast phase in the interdendritic region). The EDX analysis revealed that the eutectic phase contains about 12.6 wt.% silicon confirming it to be eutectic Si based on the phase diagram of Al-Si alloy [24, 25]. The as-cast A356-1.5TiB_2 composite sample, as shown in Figure 3d, contains prominently three phases which are continuous dark phase which is the matrix, white contrast spherically shaped phase in the interdendritic region (smaller in size) and white contrast angular phase randomly dispersed in the matrix.

The eutectic Si phase is known to be a relatively soft and brittle phase, while the α-Al dendrites are harder and ductile. The presence of the eutectic Si phase can, therefore, act as a source of weakness in the material, reducing its overall hardness and wear resistance. However, there are

ways to improve the properties of the as-cast A356 aluminium alloy. For example, heat treatment can be used to modify the microstructure of the alloy and enhance its mechanical properties. Specifically, a solution heat treatment can be used to dissolve the eutectic Si phase, which is then followed by a quenching process to produce a fine-grained microstructure. This process results in an increase in the hardness and wear resistance of the alloy due to the presence of the fine-grained microstructure, which reduces the likelihood of crack propagation and enhances the strength of material.

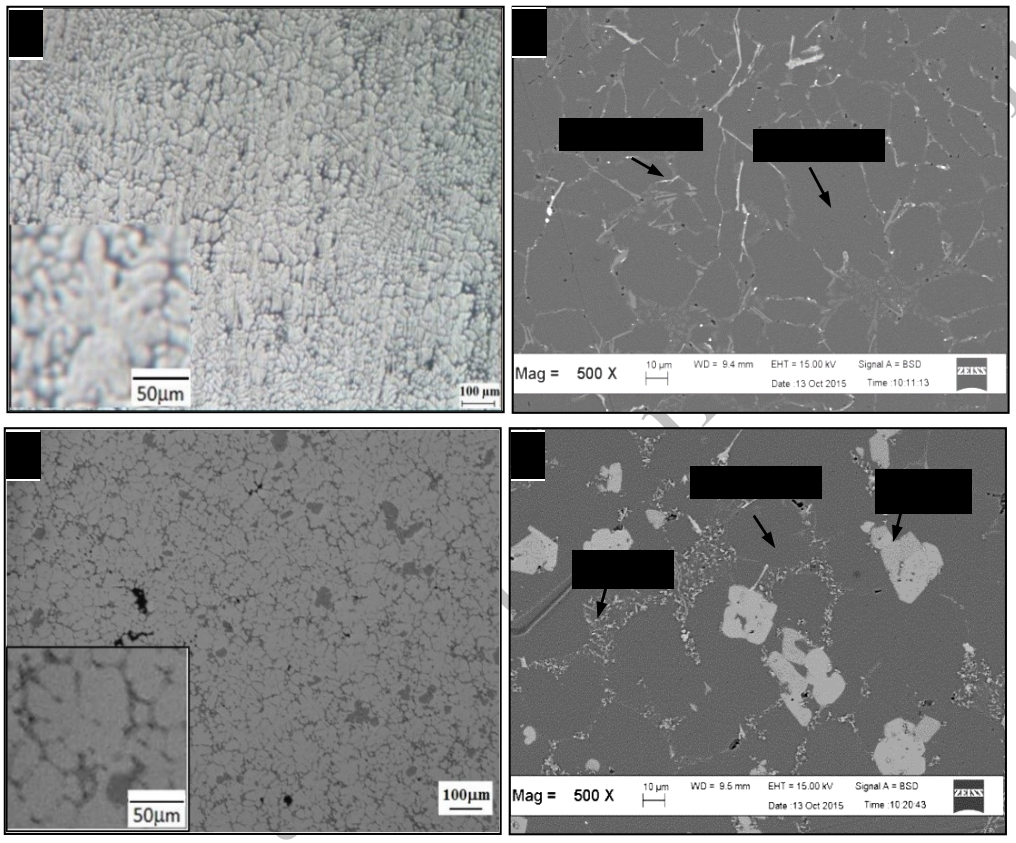

Figure 3. *Optical micrographs and SEM images of (a,b) as-cast A356 aluminum alloy, and (c,d) as-cast A356-1.5 wt.%TiB_2 composite*

The result of the XRD analysis in Figure 4 confirmed the presence of Al (ICDD Card No: 04-0787) matrix, Si (ICDD-01-089-5012), and hard particles of $TiAl_3$ (ICDD-00-37-1449) and TiB_2 (ICDD Card No: 07-0275). According to Zhao et al. [26], the white contrast angular phase randomly dispersed in the continuous Al matrix is believed to be $TiAl_3$ while the smaller sized white spherically shaped phase found in the interdendritic region is adjudged to be Si–TiB_2. According to Mandal et al. [27] and Wang et al. [28], TiB_2 particles are usually of size less than 3 µm and agglomerates at the eutectic region to form Si–TiB_2 network while $TiAl_3$ particles have a flaky or rod-like shape with size ranges from 10 µm to 40 µm.

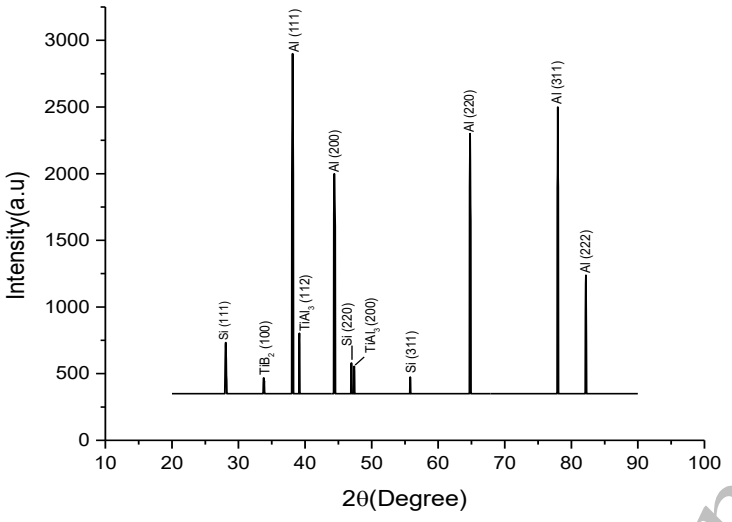

Figure 4. *XRD analysis of as-cast A356-1.5TiB_2 composite*

Mohanty and Gruzleski [29] reported that boride (TiB_2) particles are pushed to the interdendritic region by the solid–liquid interface (*S/L* interface). The insoluble TiB_2 particles act as heterogeneous nucleation sites that refine the α-Al grain [30]. TiB_2 particles reduced the length of dendritic arms and homogenized the A356 aluminum alloy grains. This explains the reduction in the average grain size of as-cast A356 from 48.8 μm to 34.8 μm after the addition of 1.5 wt.% TiB_2. The grain sizes of the sample with addition of TiB_2 are more homogenous compared with those of the as-cast A356 sample. Thus, TiB_2 particles refined the primary grains and inhibited grain growth during the solidification process producing homogeneous structures.

The microstructures of the as-cast A356-1.5wt.%TiB_2 composite post-processed in different sequences of ECAP and Aging processes (i.e. ST-ECAP, ST-Aging-ECAP and ST-ECAP-Aging), as designated in Table 1 are shown in Figure 5. The microstructures revealed that the solution treatment before ECAP caused TiB_2 and silicon to be located at the eutectic region but did not redistribute the particles in the aluminum matrix (See Figure 5a). However, Si phase and TiB_2 particles were randomly redistributed in the soft aluminum matrix after ECAP processing, as shown in Figure 5c and 5d. The ECAP processing showed no significant impact on hard $TiAl_3$ particles.

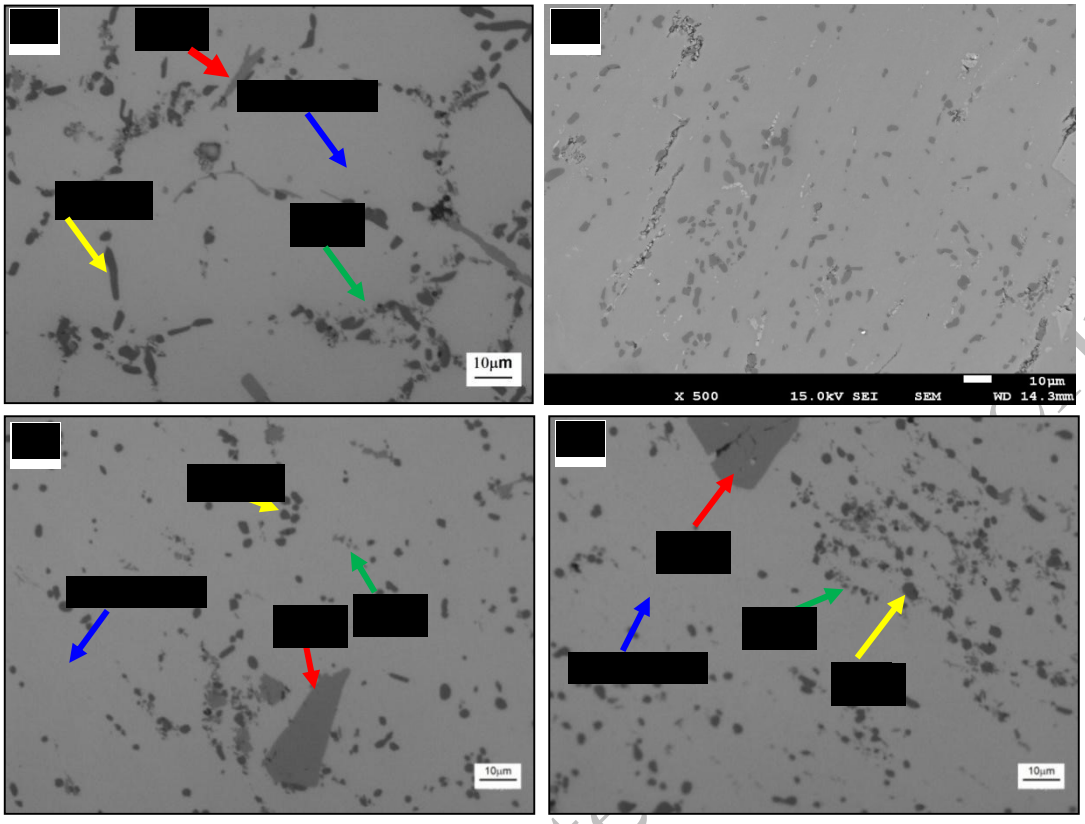

Figure 5. *Optical micrographs of A356-1.5wt.%TiB_2 composite samples showing the distribution of Si, TiB_2 and $TiAl_3$ phases in aluminium matrix after (a) solution treatment, (b) ST-ECAP, (c) ST-Aging-ECAP and (d) ST-ECAP-Aging*

3.2 EBSD Characterization

The electron backscattered diffraction (EBSD) micrographs of A356-1.5TiB_2 samples are shown in Figure 6. The EBSD analysis was performed to measure the misorientation angle of the grains. The microstructure of all the post-processed ECAP samples showed severely fragmented and elongated grains along its longitudinal direction (Figure 6 b–d). The elongated grains fragmented into sub-grains with low- and high-angle grain boundaries. The samples exhibited a bimodal grain structure with a mixture of submicron- and nano-sized grains; the large grains maintained the material deformation, while the nano- and submicron-sized grains conferred strength.

The microstructure of the ST-ECAP sample (Figure 6b) are elongated, and some are equiaxed. High amount of high-angle grain boundary (HAGBs) and low-angle grain boundary (LAGBs) was developed in the sample. This finding is due to the solution treatment before ECAP, which softened the aluminum matrix and resulted in large deformation during ECAP. The large deformation increases the misorientation in the grains due to the evolution of LAGB into HAGB. Meanwhile, the ST-Aging-ECAP sample has high fraction of LAGBs, and low fractions of HAGBs respectively. The increase in the fraction of LAGBs attributed to the development of dense dislocation walls and refined the grains [31].

The HAGBs in the ST-Aging-ECAP sample (Figure 6c) are located in areas near particles because the sample underwent precipitation hardening before ECAP. The precipitates formed during the aging process are capable of inhibiting dislocation movements during the ECAP process. Therefore, increasing the internal strain in the sample facilitates the grain refinement in the sample. The ST-ECAP-Aging sample has more LAGBs than the ST-Aging-ECAP sample as shown in Figure 6 (d). This finding is due to the softened aluminum matrix causing easy deformation of the cast composite during ECAP in the case of ST-ECAP-Aging sample. This induced high dislocation density inside the material. Subsequent aging at 155 °C for 3 hours did not alter the microstructure of the sample because the temperature is below its recrystallization temperature [32]. This indicated that the careful selection of manufacturing process enhances the properties of A356-1.5%TiB_2 particularly in achieving a finer grain size.

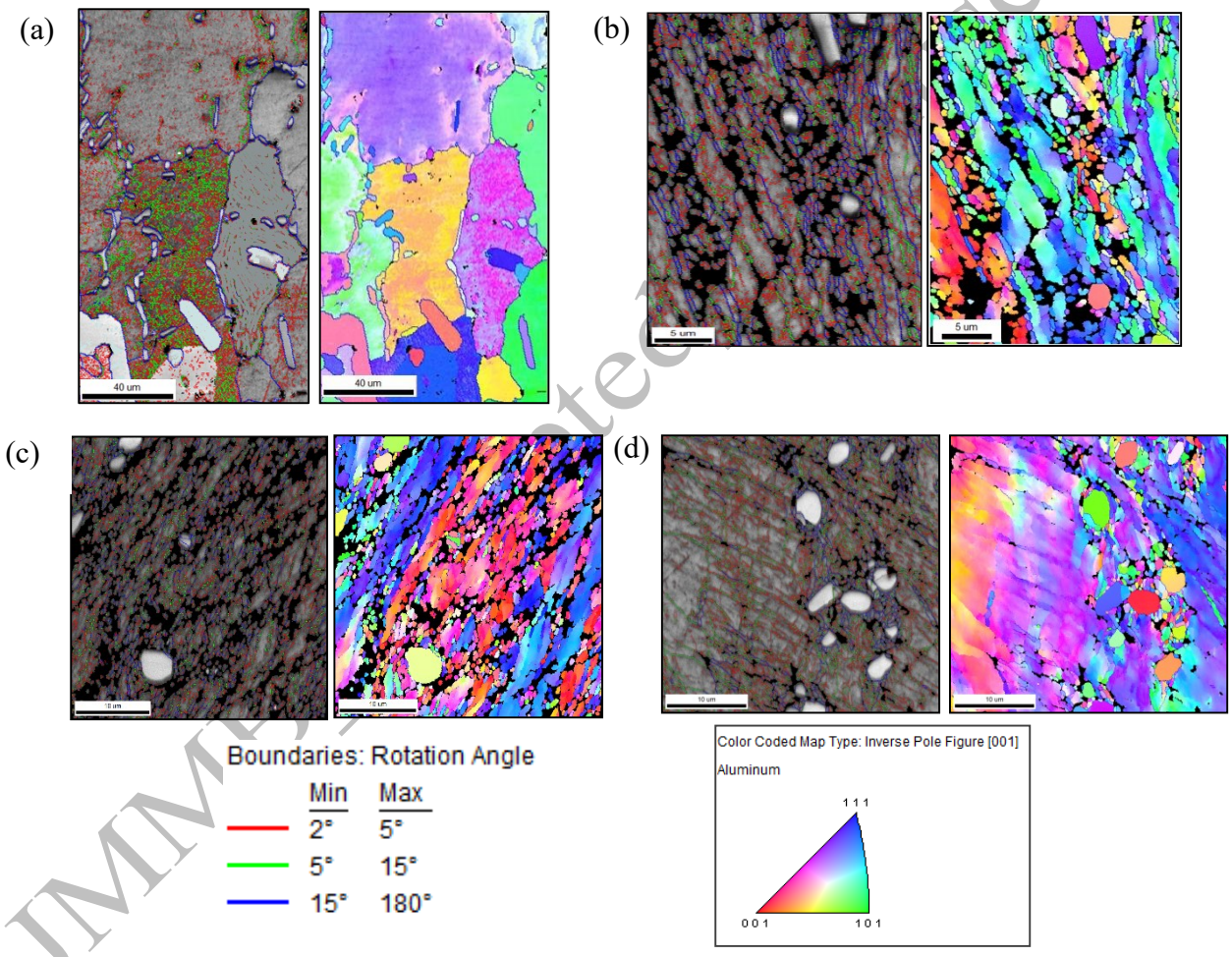

Figure 6. *Image quality (IQ) and inverse pole figure (IPF) maps of A356-1.5TiB_2 composites after (a) solution treatment, (b) ST-ECAP, (c) ST-Aging-ECAP and (d) ST-ECAP-Aging*

3.3 TEM Characterization

Transmission electron microscopic (TEM) studies were conducted to evaluate the characteristics of the deformed Al grains in the ST-ECAP and ST-Aging-ECAP samples. Due to the severe strain imposed into the material, the TEM images revealed the generation of dislocations and continuous evolution into dislocation tangles/cells for ST-ECAP and ST-Aging-ECAP samples. ST-Aging-ECAP sample shows a higher density of dislocations and presence of dislocation forests compared with that of the ST-ECAP sample. The dislocation cell structure influences the mechanical properties and the orientation of the grains [33]. TiB_2 particles with cuboidal shapes were detected in the microstructure, as shown in Figure 7 (a,b). The TiB_2 particles were found to be smaller in size for ST-Aging-ECAP sample compared with the ST-ECAP sample. These particles can provide the pinning effect to the dislocation movement. The distribution of dislocations and TiB_2 particles play a vital role towards enhancing the mechanical properties of the composite [34]. Meanwhile, the dislocations entrapped between the TiB_2 particles will also result in better mechanical properties.

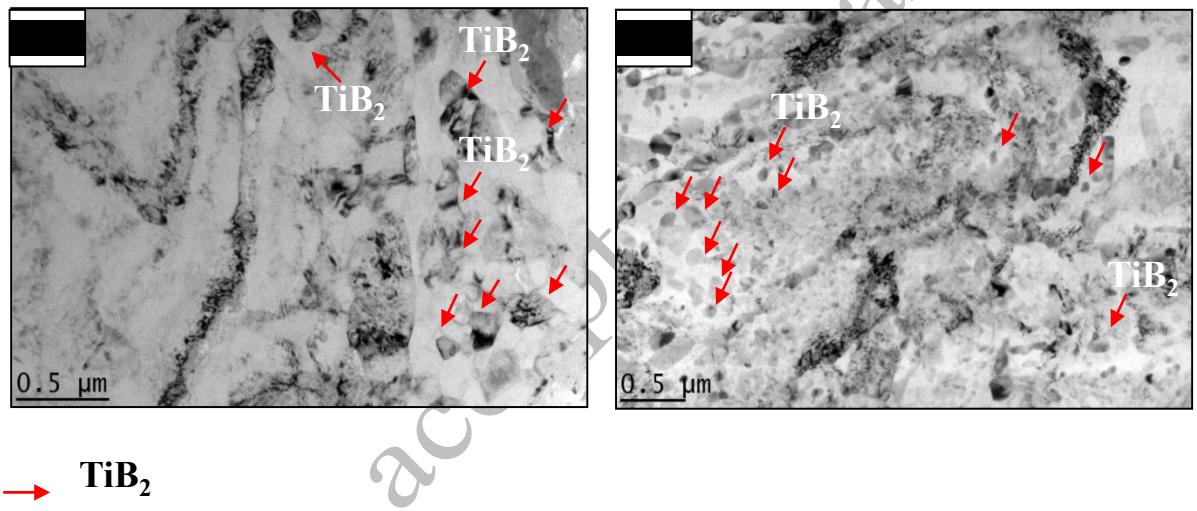

Figure 7. *TEM images of (a) ST-ECAP and (b) ST-Aging-ECAP*

3.4 Grain refinement during ECAP

LAGBs and HAGBs were generated during ECAP, as shown in Figure 8. Grain refinement generally depends on the formation and migration of LAGBs and HAGBs. The HAGB is the misorientation angle of a grain with a grain adjacent to a grain larger than 15° [35-37]. HAGBs have disordered atoms in the boundary plane, whereas LAGBs can be regarded as arrays of dislocations [38]. HAGB is represented by blue lines in all the samples. The number of points in Figure 8 indicates the TiB_2 or Si particles. The second phase TiB_2 can influence the transformation from LAGBs to HAGBs by pinning grain boundaries and dislocations [39]. Hence, the second phase is crucial in grain refinement. TiB_2 particles are reported to hinder the growth of dislocation cell structure and deformation bands, leading to a decrease in HAGBs [40]. The effect of these particles on the grain refinement, especially in the ST-Aging-ECAP sample, is observed. Fine grains with HAGBs are rapidly developed within the deformation zones surrounding the hard particles (TiB_2 and Si) due to the deformed areas around these particles, which induce high dislocation densities and then eventually refine the grains [41].

Samples processed through ECAP have shown that most of the grain sizes are between 0.2 μm and 1.1 μm. The number of grains with a size range of 0.2–1.1 μm for each ECAP sample is 83% for ST-Aging-ECAP sample, 80% for ST-ECAP-Aging sample, and 69% for ST-ECAP sample. Therefore, 4-pass ECAP processing of A356 aluminum alloy with 1.5 wt.% TiB_2 significantly refined grains. Consequently, grain refinement occurs remarkably fast in the sample containing the hard particles [41].

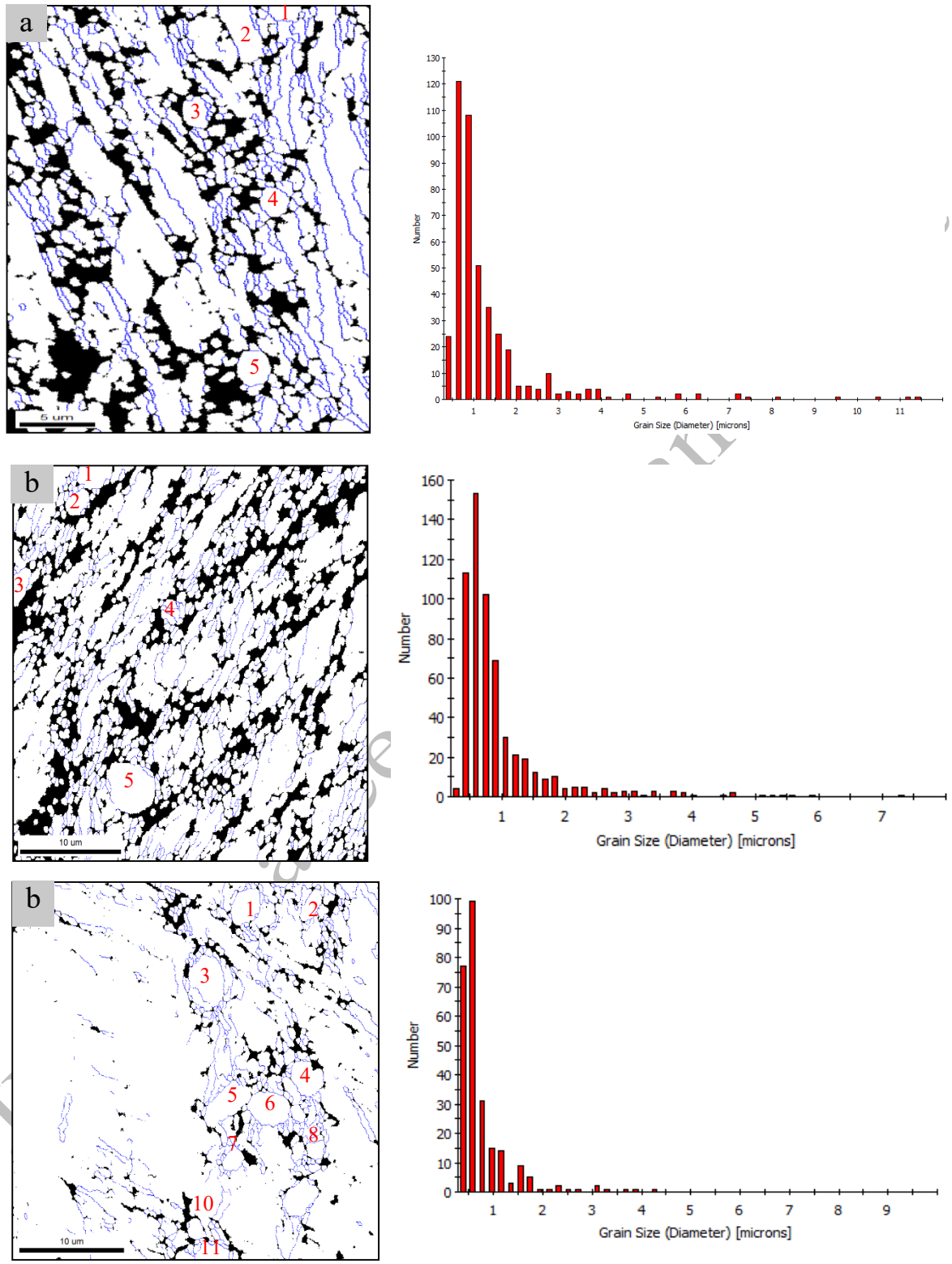

Figure 8. *HAGBs indicated with blue lines and grain distribution of (a) ST-ECAP, (b) ST-Aging-ECAP and (c) (ST-ECAP-Aging)*

3.5 Hardness

The hardness of as-cast A356 aluminum alloy with and without TiB_2 recorded a value of 68 ± 1.3 HV and 62 ± 1.3 HV. The finding is consistent with that of Lokesh and Mallik [22]. The increase in hardness after the addition of 1.5 wt.% TiB_2 is due to the presence of hard particles of TiB_2 and $TiAl_3$. In the past, Mandal et al. [27] has reported a slight increase in hardness (2.5 HV) of A356 aluminum alloy with an addition of 1.5 wt.% TiB_2. The increase in hardness was not significant because TiB_2 particles agglomerate at grain boundaries. TiB_2 particles were not well distributed in the aluminium matrix thereby limiting grain refinement action of the particles in the entire matrix.

Figure 9 presents the hardness of A356 aluminum alloy with an addition of 1.5 wt.% TiB_2 when post-processed ECAP at various processing conditions and sequence. The sample after ECAP showed improvement in hardness. The severe plastic deformation during ECAP leads to the formation of high-density dislocations and a reduction in the grain size of the material. The changes in the microstructure can lead to an increase in the hardness of the material because the presence of a large number of dislocations and a smaller grain size can hinder the motion of dislocations, which can limit the ability of the material to deform under an external load.

Among the samples, the ST-Aging-ECAP sample has the highest hardness (130 ± 1.1 HV). Two microstructural phenomena; precipitation hardening and redistribution of the TiB_2 and $TiAl_3$ might be occurred during aging treatment and ECAP [42,43]. The combined effects of the two phenomena contribute largely to the high hardness of the sample. For ST-ECAP sample (122 ± 1.4 HV), ECAP processing is the main factor determining the hardness because aging treatment was not performed for this sample. In the case of ST-ECAP-Aging sample, the hardness recorded was 124 HV. This indicated that the aging process after severe plastic deformation did not produce almost the effect as when compared with the ST-Aging-ECAP sample (130 HV). In summary, ECAP can improve the hardness of a material by inducing high-density dislocations and reducing the grain size, which can hinder the motion of dislocations and limit the material's ability to deform under an external load.

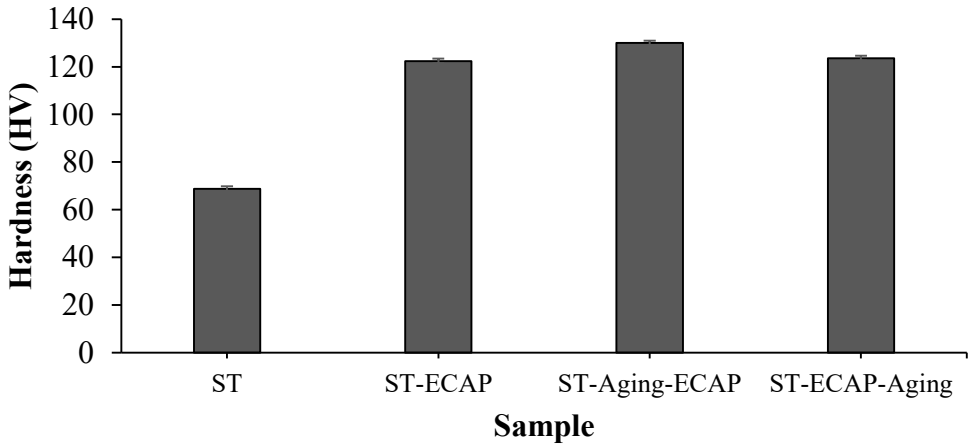

Figure 9. *Hardness of A356 aluminum alloy with 1.5 wt.% TiB_2 at various processing treatments*

3.6 Wear

Wear tests were performed for A356 samples containing 1.5 wt.% TiB_2 that underwent various processing treatments, including as-cast, ST-ECAP, ST-Aging-ECAP and ST-ECAP-Aging composite samples. The wear test of as-cast composite sample was compared with the ST-ECAP, ST-Aging-ECAP and ST-ECAP-Aging composite samples to evaluate the effect of ECAP and different heat treatments on wear behavior of A356-1.5wt.% TiB_2 composite. Figures 10 and 11 show the volume loss of the samples at applied loads of 30 and 50 N with varying sliding distances. All composite samples post-processed by ECAP and heat treatment exhibited lower volume loss (or mass loss) compared with as-cast samples at low (30 N) and high (50 N) loads. Among the post-processed composite samples, ST-ECAP sample demonstrated the lowest volume loss at an applied load of 30 N. At higher load of 50N, ST-ECAP sample shows the lowest volume loss up to 3 km sliding distance after which the ST-Aging-ECAP sample started competing with ST-ECAP sample for the lowest volume loss.

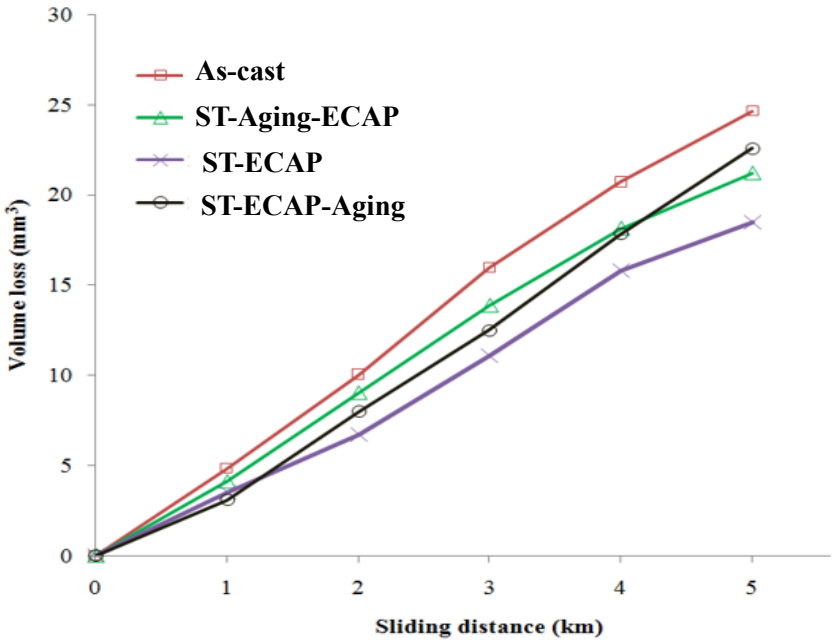

Figure 10. *Volume loss of as-cast A356-1.5 wt.%TiB_2 composite and A356-1.5 wt.%TiB_2 composite post processed by ECAP and heat treatments at varying sliding distance at a load of 30 N*

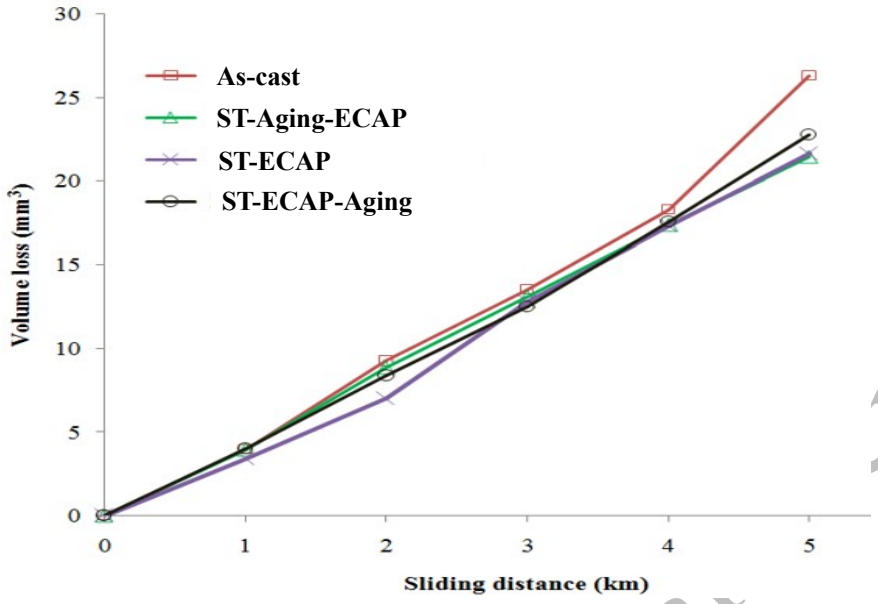

Figure 11. *Volume loss of as-cast A356-1.5 wt.%TiB_2 composite and A356-1.5 wt.%TiB_2 composite post processed by ECAP and heat treatments at varying sliding distance at a load of 50 N*

Lower volume loss demonstrated by all post-processed composite samples compared with the as-cast composite sample is an indication that the post-processed samples have higher wear resistance than the as-cast composite sample. The reason for higher resistance can be traced to the better particle distribution, finer grain structure and higher hardness demonstrated by the post- processed samples [44, 45].

The morphology of the particles in the alloy matrix is another factor that influences wear resistance. Though all the A356-1.5wt.% TiB_2 composite samples contain hard secondary phases including $TiAl_3$ and TiB_2, and also Si-phase, the TiB_2 particles and Si-phase are in the form of eutectic Si–TiB_2 networks which are interconnected at the grain boundary in the as cast composite. The hard but brittle eutectic networks are easy to crack during wear tests and detach from the Al matrix resulting in three-body abrasive wear. This explains the reason for the relatively higher weight loss exhibited by the as-cast composite. The eutectic networks in the heat treated and ECAP post-processed composites were divided into TiB_2 and Si due to heat treatment, and both particles were well dispersed in the aluminum matrix due to ECAP processing. Consequently, the abrasive action of these particles decreases during the wear test, leading to reduced weight loss at both high and low load conditions [46].

The specific wear rate (S_{WR}) of all the tested samples decreased with increasing load, as shown in Figure 12. Both abrasive and adhesive wear mode were observed in the tested samples. The adhesive wear mode was mainly experienced by all ECAP-processed composites as indicated by the transfer of the sample material to the counter disk. The material transfer was visibly attached to the surface of the counter disk at several points along the sliding path during the wear test. The worn surface of adhesive wear is normally characterized by a tribolayer, which generally

comprises plastically deformed and oxidized particles, thereby reducing the wear rate of the wear test sample [47]. The competition between the transfer of material attached to the counter disc and the tribolayer determines the overall wear resistance of the sample. In the case of as-cast sample, predominantly abrasive wear indicated by a considerable number of small debris formed during the wear test, and no significant material was attached to the counter disk due to adhesive wear. The specific wear rate of the as-cast sample is highest due to the predominant occurrence of the abrasive wear occur.

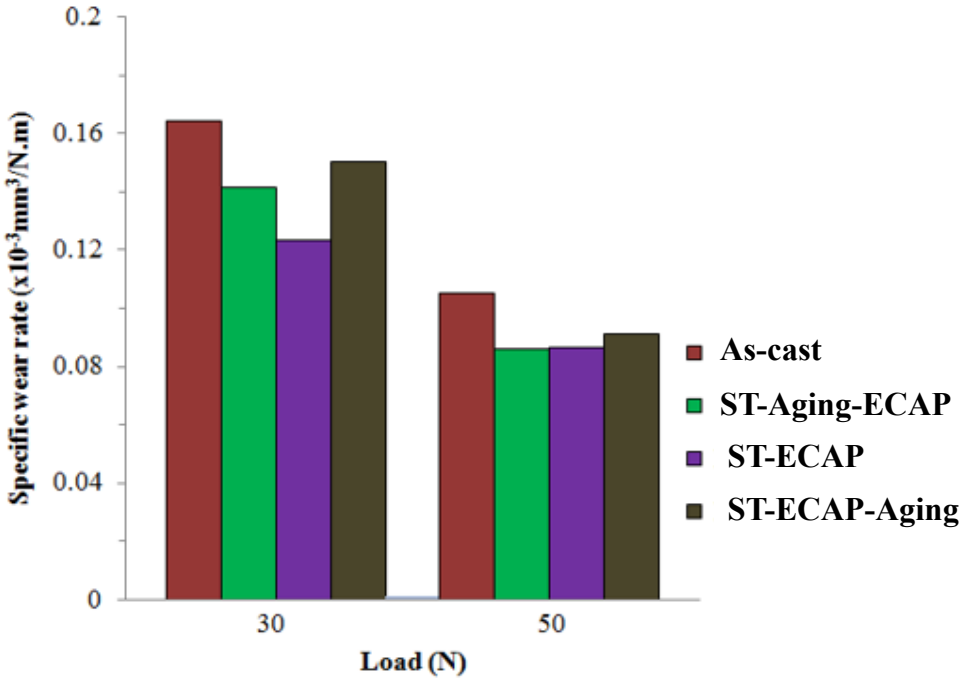

Figure 12. *Specific wear rate of as-cast A356-1.5 wt.%TiB_2 composite and A356-1.5 wt.%TiB_2 composite post processed by ECAP and heat treatments at different loads (30 and 50 N)*

The worn surface morphology of the as-cast sample is characterized by scratches, mild delamination, and predominantly pit/groove formation, as depicted in Figure 13(a). These features indicate a gross transfer of material and are consistent with the abrasive wear mechanism. Abrasive wear typically involves three mechanisms, namely micro cutting of the matrix, plastic deformation resulting from plowing action, and fracture of the reinforcement particles [48, 49]. The presence of grooves on the worn surface is indicative of this abrasive wear mechanism. The large grooves observed on the as-cast composite sample are caused by the fracture of the eutectic Si–TiB_2 networks, which makes it easier to remove the hard and brittle phases from the aluminum matrix. Additionally, the matrix phase is relatively softer since it has not undergone any aging treatment to harden it. As a result, the harder wear disc can more easily degrade the softer matrix, and this effect is particularly pronounced at higher loading conditions (50 N).

The post-processed ECAP samples were largely dominated by delamination wear (see Figure 13b, c and d), which occurs due to plastic deformation. Plastic deformation begins with softening of the sample surface due to the heat generated by friction, and then the softened surface is sheared by mating surfaces. There is no significant evidence of large groove or pit formation. Therefore,

ECAP processing improves the wear resistance of A356-1.5wt.% TiB_2 composite regardless of heat treatment sequence.

Among the post-processed composite samples, the lowest wear rate demonstrated by the ST-ECAP composite sample might be due to the homogeneous distribution of particles (TiB_2) during solution treatment and the good bonding of TiB_2 particles with the Al 356 alloy matrix. The presence of other precipitates (due to aging) and TiB_2 increased the hardness of the ST-Aging-ECAP and ST-ECAP-Aging samples. However, these precipitates, which are concentrated near TiB_2 particles, is adjudged to have blocked the dislocation motion. This phenomenon may have led to weakening/debonding between TiB_2, precipitate, and the Al matrix during the wear test. This may have led to removal of more materials (TiB_2) from the matrix [20].

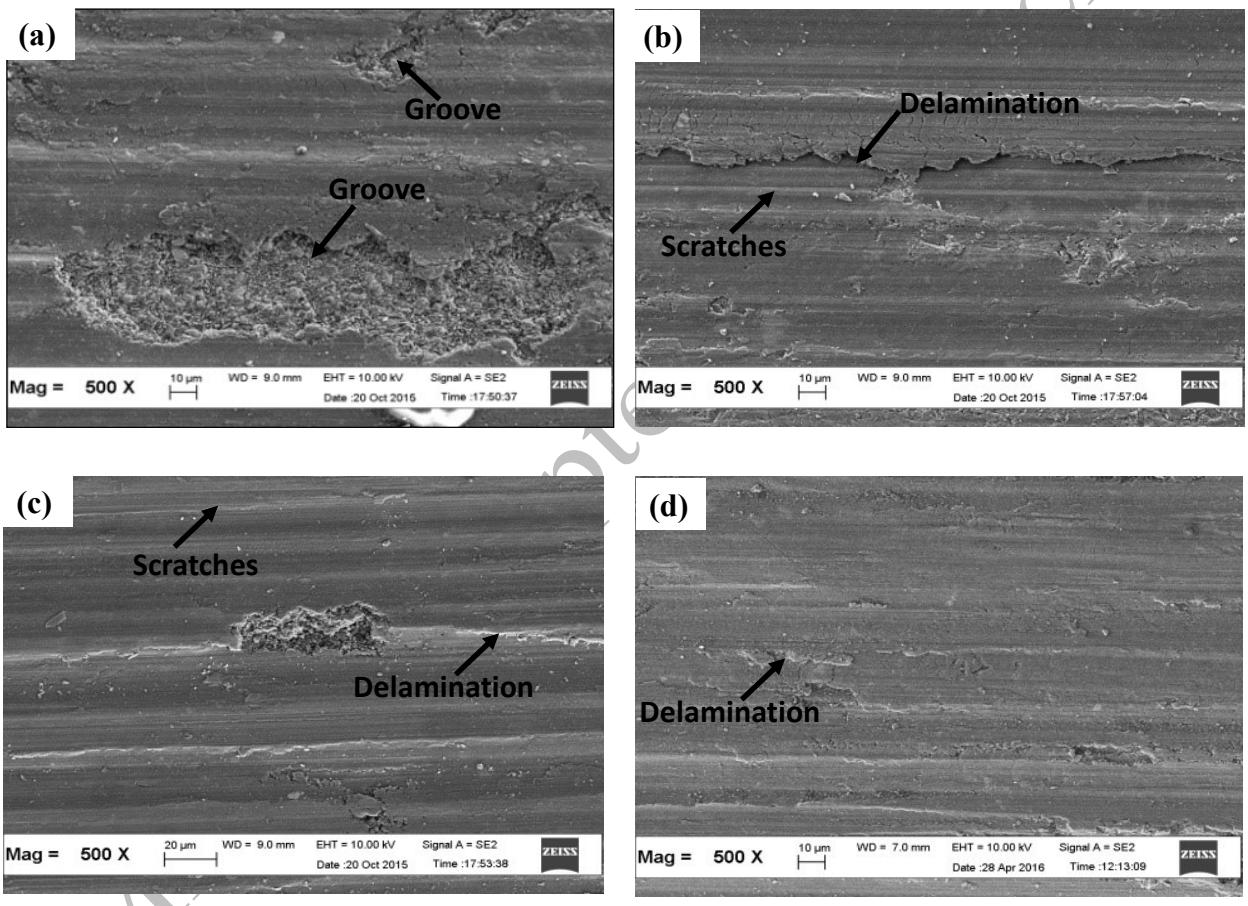

Figure 13. *SEM images of worn surfaces of (a) as cast, (b) solution treatment + 4-pass ECAP (ST-ECAP) (c) solution treatment + Aging + 4-pass ECAP (ST-Aging-ECAP) and (d) solution treatment + 4-pass ECAP + Aging (ST-ECAP-Aging) A356-1.5 wt.% TiB_2 composite*

4.0 Conclusion

The effect of ECAP and heat treatment sequence on the cast A356-1.5wt.% TiB_2 composite has been successfully investigated and the following conclusions were drawn:

- The addition of 1.5 wt.% TiB_2 to as-cast A356 aluminum alloy resulted in the formation of $TiAl_3$ and TiB_2 hard phases (particles) which eventually refined the A356 grain structure and improved its hardness.
- The post applications of ECAP and heat treatment processes resulted in increased hard particles distribution homogeneity, significant improvement in hardness and wear resistance of the A356-1.5TiB_2 composite.
- A356-1.5TiB_2 composite post processed by both ECAP and aging treatments demonstrated finer grain structure and hardness than the composite sample post-processed by ECAP only.
- The aging heat treatment sequence influences the degree of grain refinement, hardness improvement in the A356-1.5TiB_2 composite.
- A356-1.5TiB_2 composite post-processed by solution treatment followed by aging treatment and then ECAP demonstrated the most refined structure and highest hardness.
- A356-1.5TiB_2 composite post-processed by solution treatment and then ECAP demonstrated the lowest wear rate.

Acknowledgments
The authors gratefully acknowledge the financial support from Japan International Cooperation Agency-ASEAN University Network/Southeast Asia Engineering Education Development Network (JICA AUN/SEED-Net).

Author Contributions
Muhammad Syukron - Draft manuscript preparation, A.S.Anasyida – design and supervision, H.Zuhailawati - analysis and interpretation of results, M.H.Hassan – editing manuscript, B.K. Dhindaw- critical review, S.A.Zakaria - formatting manuscript, T.E.Abioye - editing manuscript. All authors reviewed the results and approved the final version of the manuscript.

Disclosure of Conflict of Interest
The authors have no disclosures to declare.

Compliance with Ethical Standards
The work is compliant with ethical standard.

References
[1] N.Gangil, A.N.Siddiquee, S.Maheswari, Aluminium based in-situ composite fabrication through friction stir processing: A review, Journal of Alloys and Compounds, 25 (2017) 686-690. http://dx.doi.org/10.1016/j.matpr.2019.08.062.
[2] T.Abioye, H.Zuhailawati, A.S.Anasyida, S.Ayodeji, P.Oke, Effects of particulate reinforcements on the hardness, impact and tensile strengths of AA 6061-T6 friction stir weldments, Proceedings of the Institution of Mechanical Engineers, Part L: Journal of Materials: Design and Applications, 235 (6) (2021) 1500–1506. https://doi:10.1177/1464420721995544.
[3] K.M.Shorowordi, T.Laoui, A.S.M.A.Haseeb, J.P.Celis, L.Froyen, Microstructure and interface characteristics of B_4C, SiC and Al_2O_3 reinforced Al matrix composites: a comparative study, Journal of Materials Processing Technology, 142 (3) (2003) 738-743. https://doi:10.1016/S0924-0136(03)00815-X.

[4] K.Kaviyarasan, S.Thiyagu, V.Shabari, R.Saileswaran, S.Siva Sankaran, T.Sivanesan, Investigation on mechanical properties of aluminium alloy A356 by reinforcing with TiB_2 & WC composites, IOP Conference Series: Materials Science and Engineering, 1145 (2021) 012110. https://doi:10.1088/1757-899X/1145/1/012110.
[5] A.Ali Gad El-Mawla, S.El-Abden, H.Badran, Wear Behaviour of Al6061/TiO_2 Composites Synthesized by Stir Casting Process, International Journal of Advanced Research Trends in Engineering and Technology, 41(2) (2021) 113-125. https://doi:10.21608/JAET.2021.55413.1081.
[6] H.Abdizadeh, H.R.Baharyandi, K.Shirvani Moghaddam, Comparing the effect of processing temperature on microstructure and mechanical behaviour of ($ZrSiO_4$ or TiB_2)/aluminum composites, Materials Science and Engineering A, 498 (2008) 53-58. https://doi:10.1016/j.msea.2008.07.009.
[7] R.Arunbharathi, V.P.Ashoka, J.S.C.Samson, Investigation on mechanical properties and dry sliding wear characterization of stir cast LM13 aluminium alloy-ZrB_2-TiC particulate hybrid composites, Material Research Express, 6(6) (2019) 066578. https://doi: 10.1088/2053-1591/ab0ef8.
[8] P.Aasiya P, Nathi Mohd Suhaib, Influence of compaction pressure and Si_3N_4/ZrO_2 reinforcement on the properties of aluminium hybrid composites, Advance Material Process Technology 8 (3) (2021) 1-13. https://doi:10.1080/2374068X.2021.1945289.
[9] A.Bhowmik, D.Dey, A.Biswas, Comparative study of microstructure, physical and mechanical characterization of SiC/TiB_2 reinforced aluminium matrix composite, Silicon 13 (2021) 2003-2010. https://doi:10.1007/s12633-020-00591-2.
[10] C.T.Lee, S.W.Chen, Quantities of grains of aluminum and those of TiB_2 and Al_3Ti particles added in the grain-refining processes, Material Science Engineering A, 325 (1-2) (2021) 242–248. https://doi:10.1016/s0921-5093(01)01464.
[11] M.Guzowski, G.K.Sigworth, D.A.Sentner, The role of boron in the grain refinement of aluminium with titanium, Metallurgy Transaction A, 18 (1987) 603-619. https://doi.org/10.1007/BF02649476.
[12] R.G.Guan, D.Tie, A Review on grain refinement of aluminum alloys: progresses, challenges and prospects, Acta Metallurgica Sinica (English Letters), 30(5) (2017) 409–432. https://doi:10.1007/s40195-017-0565-8.
[13] C.Wang, A.Ma, J.Sun, H.Liu, H.Huang, Z.Yang, J.Jiang, Effect of ECAP process on as-cast and as-homogenized Mg-Al-Ca-Mn alloys with different Mg_2Ca morphologies, Journal of alloys Compound, 793 (2019) 259–270. https://doi:10.1016/j.jallcom.2019.04.2
[14] S.Prithivirajan, G.M.Naik, S.Narendranath, V.Desai, Recent progress in equal channel angular pressing of magnesium alloys starting from Segal's idea to advancements till date – A review, International Journal of Lightweight Materials and Manufacture, 6 (1) (2023) 82-107. https://doi.org/10.1016/j.ijlmm.2022.08.001.
[15] A.A. Seman, S.A. Zakaria, M.S. Ahmad, Z. Hussain, B.K. Dhindaw, T.E.Abioye, Characterization of cryorolled low carbon steel using ferrite-martensite starting microstructure, Journal of Mining and Metallurgy, Section B: Metallurgy, 59 (3) (2023) 443-454. http://dx.doi.org/10.2298/JMMB230307038Z.
[16] W.Wei, R.Y.Mao, K.X.Wei, I.V.Alexandar, J.H.Hu, Effect of equal channel angular pressing on microstructure and grain refining performance of Al–5%Ti master alloy, Material Science and Engineering A, 564 (2013) 92-96. https://doi:10.1016/j.msea.2012.11.082.

[17] K.X.Wei, Y.W.Zhang, W.Wei, X.Liu, Q.B.Du, I.V.Alexandrov, J. Hu, Enhancing grain refinement efficiency and fading resistance of Al–B master alloys processed by equal channel angular pressing, Journal of Materials Research, 33 (12) (2018) 1782–1788. https://doi:10.1557/jmr.2018.95.
[18] Z.Zhang, S.Hosoda, I.S.Kim, Y.Watanabe, Grain refining performance for Al and Al–Si alloy casts by addition of equal-channel angular pressed Al–5 mass% Ti alloy, Material Science and Engineering A, 425 (2006) 55-63. https://doi:10.1016/j.msea.2006.03.018.
[19] A.Chidambaram, S.Balasivanandha Prabu, K.A.Padmanabhan, Microstructure and mechanical properties of AA6061–5wt. %TiB_2 in-situ metal matrix composite subjected to equal channel angular pressing, Material Science and Engineering A, 759 (2019) 762-769. https://doi: 10.1016/j.msea.2019.05.068.
[20] A.Chidambaram, A.S.Vivekananda, S.Balasivanandha Prabu, K.A.Padmanabhan, On the wear behaviour of AA6061 alloy and in-situ AA6061-TiB_2 composite subjected to Equal Channel Angular Pressing, Surface Topography: Metrology and Properties, 8 (4) (2020) 045005. https://doi:10.1088/2051-672X/abbb80.
[21] R.Shobha, C.Siddaraju, K.R.Suresh, H.B.Niranjan, mechanical property evaluation of heat treated insitu Al- TiB_2 composite after severe plastic deformation, Material Today Proceedings, 5 (2018) 2534-2540. https://doi:10.1016/j.matpr.2017.11.036.
[22] T.Lokesh, U.Mallik, Effect of ECAP process on the microstructure and mechanical properties of Al6061-Gr composites, Materials Today, 5 (1) (2018) 2453–2461. https://doi:10.1016/j.matpr.2017.11.025.
[23] T.E.Abioye, H.Zuhailawati, A.S.Anasyida, S.A.Yahaya, M.N.F.Hilmy, Enhancing the surface quality and tribomechanical properties of AA 6061-T6 friction stir welded joints reinforced with varying SiC contents, Journal of Materials Engineering and Performance, 30(6) (2021) 4356–4369. https://doi:10.1007/s11665-021-05760-x.
[24] M.Chakrabortyl, A.Mandal, G.S.Vinod Kumar, K.R.Ravi, I.G.Siddhalingeshwar, R.Mitra, B.S.Murty, Recent developments in aluminium alloy reinforced titanium diboride in-situ composites, Indian Foundry Journal, 58 (2019) 29-34. https://doi:10.1007/s11665-015-1424-2.
[25] K.Oh-ishi, Y.Hashi, A.Sadakata, K.Kaneko, Z.Horita, T.G.Langdon, Microstructure control of an Al–Mg–Si alloy using equal-channel angular pressing, Materials Science Forum, 396-402 (2002) 333-338. https://doi:10.4028/www.scientific.net/msf.396-402.333.
[26] Y.Zhao, Z.Lu, L.Mi, Z.Hu, W.Yang, Morphological evolution of TiB_2 and $TiAl_3$ in Al–Ti–B master alloy using different ti adding routes, Materials (Basels), 15(6) (2022) 1984. https://doi: 10.3390/ma15061984.
[27] A.Mandal, M.Chakaborty, B.S.Murty, Aging behaviour of A356 alloy reinforced with in-situ formed TiB_2 particles, Material Science and Engineering A, 489 (2008) 220-226. https://doi:10.1016/j.msea.2008.01.042.
[28] T.Wang, Y.Zhao, Z.Chen, Y.Zheng, H.Kang, Combining effects of TiB_2 and La on the aging behaviour of A356 alloy, Material Science and Engineering A, 644 (2015) 425-430. https://doi:10.1016/j.msea.2015.07.076.
[29] P.S.Mohanty, and J.E.Gruzleski, Grain refinement mechanisms of hypoeutectic Al-Si alloys, Acta Materialia, 44 (9) (1996) 3749-3760. https://doi.org/10.1016/1359-6454(96)00021-3.
[30] X.Dong, S.Ji, Grain refinement of Al–Si–Mg cast alloys by Al_3Ti_3B master alloy, Minerals, Metals and Materials Series, (2018) 319-323. http://dx.doi.org/10.1007/978-3-319-72284-943.

[31] X.Sauvage, G.Wilde, S.V.Divinski, Z.Horita, R.Z.Valiev, Review: Grain boundaries in ultrafine grained materials processed by severe plastic deformation and related phenomena, Material Science and Engineering A, 540 (2012) 1-12. https://doi:10.1016/j.msea.2012.01.080.
[32] G.E.Totten, D.S.MacKenzie, Handbook of Aluminium: Physical Metallurgy and Processes, 1 Marcell Dekker, 2013, pp. 259-262.
[33] S.K.Ramesh, G.Kondaiah, B.Tejaswi, Effect of microstructure and mechanical properties of Al–Mg alloy processed by ECAP at room temperature and cryo temperature, Transactions of the Indian Institute of Metals, 70(3) (2017) 639-648. https://doi: 10.3390/cryst11060683.
[34] R.Du, Q.Gao, S.Wu, S.Lu, X.Zhou, Influence of TiB_2 particles on aging behaviour of in-situ TiB2/Al-4.5Cu composites, Material Science and Engineering A, 721 (2018) 244-250. https://doi.org/10.1016/j.msea.2018.02.099.
[35] J.R.Bowen, O.V.Mishin, P.B.Prangnell, D.J.Jensen, Orientation correlations in aluminium deformed by ECAE, Scripta Materialia, 47 (2002) 289-294. https://doi.org/10.1016/S1359-6462(02)00109-4.
[36] P.W.J.Mckenzie, R.Lapoyok, ECAP with back pressure for optimum strength and ductility in aluminium alloy 6061. Part 1: Microstructure, Acta Materialia, 58 (2010) 3198-3211. https://doi: 10.1016/j.actamat.2010.01.038.
[37] D.A.Hughes, and N.Hansen, High angle boundaries formed by grain subdivision mechanisms, Acta Materialia, 45(9) (1997) 3871-3886. https://doi:10.1016/S1359-6454(97)00027-X.
[38] R.Abbaschian, L.Abbaschian, and R.E.Reed-Hill, Physical metallurgy principles, Cengage learning, 2010, pp. 216-218.
[39] R.Guan, R.D.K.Misra, S.Yingqhu, A.Yanan, W.Yuxiang, Z.Yang, T.Di, Mechanism of microstructural refinement of deformed aluminum under synergistic effect of TiAl3 and TiB2 particles and impact on mechanical properties, Material Science and Engineering A, 30(5) (2018) 409–432. https://doi.org/10.1016/j.msea.2018.01.043.
[40] C.Y.Dan, Z.Chen, G.Ji, S.Zhong, Y.Wu, F.Brisset, H.Y.Wang, V.Ji, Microstructure study of cold rolling nanosized in-situ TiB2 particle reinforced Al composites, Material Design, 130 (2017) 357-365. https://doi.org/10.1016/j.matdes.2017.05.076.
[41] P.J.Apps, J.R.Bowen, P.B.Prangnell, The effect of coarse second-phase particles on the rate of grain refinement during severe deformation processing, Acta Materialia, 200351 (2003) 2811-2822. https://doi:10.1016/S1359-6454(03)00086-7.
[42] P.Venkatachalam, S.R.Kumar, B.Ravisankar, V.T.Paul, M.Vijayalakshmi, Effect of processing route on microstructure and mechanical properties of 2014 Al alloy processed by equal channel angular pressing, Transactions of Nonferrous Metals Society of China, 20(10) (2010) 1822-1828. https://doi:10.1016/S1003-6326(09)60380-0.
[43] J.Wen-ming, F.Zi-tian, L.De-jun, Microstructure, tensile properties and fractography of A356 alloy under as-cast and T6 obtained with expendable pattern shell casting process, Transaction Nonferrous Metals Society of China, 22 (2012) 7-13. https://doi: 10.1016/S1003-6326(12)61676-8.
[44] I.A.Ovid'ko, A.G.Sheinerman, and N.V.Skiba, Elongated nanoscale voids at deformed special grain boundary structures in nanocrystalline materials, Acta Materialia 59 (2011). https://doi: 10.1016/j.actamat.2010.10.005.
[45] M.I.Abd El Aal, N.El Mahallawy, F.A.Shehata, M.Abd El Hameed, E.Y.Yoon, H.S.Kim, Wear properties of ECAP-processed ultrafine grained Al-Cu alloys. Mater Sci Eng A, 527(16-17) (2010) 3726-3732. htpps://doi:10.1016/j.msea.2010.03.057.

[46] S.Wilson, and A.T.Alpas, Wear mechanism maps for metal matrix composite, Wear, 212 (1997) 41-49. https://doi.org/10.1016/S0043-1648(97)00142-7.
[47] Stachowiak GW (2005) Wear: Materials, mechanism and practice, John Wiley & Sons 2005, pp. 19-22.
[48] T.E.Abioye, H.Zuhailawati, A.S.Anasyida, S.A.Yahaya, B.K.Dhindaw, Investigation of the microstructure, mechanical and wear properties of AA6061-T6 friction stir weldments with different particulate reinforcements addition, Journal of Material Research and Technology, 8 (5) (2019) 3917-3928. https://doi:10.1016/j.jmrt.2019.06.055.
[49] A.Mandal, B.S.Murty, M.Chakraborty, Sliding wear behaviour of T6 treated A356–TiB_2 in-situ composites, Wear, 266 (2009) 865-872. https://doi:10.1016/j.wear.2008.12.011.